water

MDPI

Article

Nutrient Recovery via Struvite Precipitation from Wastewater Treatment Plants: Influence of Operating Parameters, Coexisting Ions, and Seeding

Andreia F. Santos [1], Luísa S. Mendes [1], Paula Alvarenga [2], Licínio M. Gando-Ferreira [1] and Margarida J. Quina [1,*]

[1] CERES, Department of Chemical Engineering, University of Coimbra, 3030-790 Coimbra, Portugal; affs@eq.uc.pt (A.F.S.); lferreira@eq.uc.pt (L.M.G.-F.)
[2] LEAF—Linking Landscape, Environment, Agriculture and Food Research Center, Associate Laboratory TERRA, School of Agriculture, University of Lisbon, Tapada da Ajuda, 1349-017 Lisboa, Portugal; palvarenga@isa.ulisboa.pt
* Correspondence: guida@eq.uc.pt

Abstract: Phosphorus (P) is a critical element for life, and wastewater treatment systems can be strategic points for its recovery, thereby avoiding eutrophication pollution in nature. The aim of this research was to investigate P recovery via struvite, namely in terms of the influence of operating parameters, coexisting interfering ions, and seeding. This paper focuses on synthetic solutions, although an assessment was performed on wastewater. The results of the assessment indicated that, in the synthetic solution, the minimum concentration for struvite precipitation is about 30 mg P/L, and that the Mg/P molar ratio of 1 promotes P removal efficiency with less contribution from other minerals. In order to assess the results in terms of real-world scenarios, the influence of coexisting ions (calcium and sodium) was investigated. Calcium was shown to have the greatest impact on the process, as 80% was removed for an initial concentration of 200 mg Ca/L. Indeed, these experiments generated an amorphous precipitate that did not contain struvite. The utilization of biomass ash (size < 63 μm) as seeding in crystallization increased the P removal efficiency compared to the sample without seed and helped to control the pH. The precipitation experiments with wastewater demonstrated good P removal efficiencies (over 90%) but indicated a reduction in the purity of the final product (struvite was a minor crystalline phase identified in XRD—15%wt).

Keywords: phosphorus; wastewater; crystallization; struvite; crystallization seeding

Citation: Santos, A.F.; Mendes, L.S.; Alvarenga, P.; Gando-Ferreira, L.M.; Quina, M.J. Nutrient Recovery via Struvite Precipitation from Wastewater Treatment Plants: Influence of Operating Parameters, Coexisting Ions, and Seeding. *Water* **2024**, *16*, 1675. https://doi.org/10.3390/w16121675

Academic Editor: Daniel Mamais

Received: 16 May 2024
Revised: 4 June 2024
Accepted: 7 June 2024
Published: 12 June 2024

1. Introduction

The presence of nutrients in wastewater, namely phosphorus (P), is a matter of concern when released into the environment in excess (e.g., 10 μg P/L according to the United States Environmental Protection Agency (US EPA)) due to the deleterious consequences in natural ecosystems, mainly related to eutrophication [1]. Factors, such as changes in diet, the constant increase in world population, and the expansion of biofuel production, are key aspects that will significantly impact agriculture, putting pressure on P losses in the value chain. Since P is an indispensable nutrient for plant growth, the element is critical for maintaining agricultural production in optimized conditions. Several industries use P to produce specific chemicals and, in particular, to produce fertilizer [2]. Indeed, P belongs to the new 2023 Critical Raw Materials list for the European Union [3]; it is therefore imperative to develop effective and low-cost techniques to promote its recovery from different locations with relevant concentrations, including wastewater treatment plants (WWTP), and to promote circular economy models.

Phosphorus recovery as magnesium ammonium phosphate hexahydrate (MAP, $MgNH_4PO_4{\cdot}6H_2O$), commonly known as struvite, is a well-known chemical precipitation method for P recovery (and consequently nitrogen, N) used in several industrial

applications. MAP is the most common and stable form of struvite and is characterized by a crystalline and orthorhombic prismatic structure [4]. The formation of struvite (Equation (1)) occurs when the concentration of the compounds exceeds the solubility product (K_{sp}) of this mineral:

$$Mg^{2+} + NH_4^+ + H_nPO_4^{(3-n)-} + 6H_2O \rightarrow MgNH_4PO_4{\cdot}6H_2O + nH^+ \quad (1)$$

where n = 0, 1 or 2.

Several studies have been carried out to determine the K_{sp} of struvite; however, the values reported in the literature vary significantly, depending on the experimental conditions tested (namely, pH, ionic strength, temperature, etc. [5]. For example, Bube [6] determined that $K_{sp} = 10^{-12.60}$ (using the minimum concentration of Mg^{2+}, NH_4^+, and PO_4^{3-} possible to precipitate struvite), whereas Ohlinger et al. [7] indicated that $K_{sp} = 10^{-13.26}$ (at 25 °C, pH 10.7).

The main benefit of recovering P via the chemical precipitation of struvite is the production of a valuable product with high fertilizer value (containing both P and N) and low environmental risk. Indeed, its capacity to act as a slow-release fertilizer enables the soil to absorb nutrients at a slower rate while meeting plant demand and maintaining growing yields. Consequently, this feature reduces excess nutrient run-off and environmental P losses [8,9]. For the recovery of P from wastewater, it is important to consider that P can be present in different chemical compounds with different reactivities, and the potential interference of conditions in the wastewater must be taken into account [10,11]. Indeed, struvite precipitation may remove about 80–90% of soluble reactive phosphorus (the total P fraction that is readily available for chemical reactions via coulombic attraction to cations—e.g., orthophosphates) and 20–30% of nitrogen in the wastewater. Nevertheless, this process faces at least two challenges: (i) a minimum removal efficiency of 60–70% and a concentration of 50 mg P/L are recommended to promote an economic, environmental, and operationally viable process [12–14], and (ii) Mg concentration in wastewater is typically low, requiring an external source. Moreover, several other parameters influence the formation of struvite such as pH, Mg/P molar ratio, Mg source, ionic strength, and temperature. Some of these variables can be controlled and optimized, while the most critical aspect tends to be the presence of competitive ions. The wastewater is a complex matrix with several other ions (e.g., Na^+, Ca^{2+}, and others) that may have an impact on the nucleation and growth of struvite crystals in terms of morphology and size. These ions can hinder the efficiency of P recovery and the purity of the product [4,5,15–17]. According to the literature, calcium seems to be the most problematic element because of the possibility of forming hydroxyapatite or calcium phosphates, thereby reducing struvite purity [18].

Another alternative to optimizing the process and increasing product quality is the seeding phenomenon [19]. Several methods have been explored to enhance struvite production and facilitate mineral precipitation. The seeding phenomenon with different types of seeds has been investigated to achieve quicker crystal formation and improve P removal. The formation of struvite can be described in two principal phases: nucleation and crystal growth. The nucleation is the first phase to obtain struvite crystal and can be categorized as primary or secondary nucleation depending on the type of solution used to induce the crystal formation. The primary nucleation occurs when the solution used does not contain crystalline solids. The secondary nucleation occurs in the presence of crystalline solids of the same materials that it intends to crystallize. Considering that nucleation is a spontaneous process that is crucial for the development of crystals, its optimization is relevant. In this sense, the scientific community is now turning its attention to the seeding phenomenon, which replaces the initial nucleation phase. This process involves the addition of pre-formed crystals that provide multiple mature nuclei, decreasing the energy required for nucleation [20].

Within this scope, and due to the relevance of recovering P from wastewaters, this work aims to complement studies in the literature about the precipitation of struvite in terms of (i) studying the kinetics of removing P in different operating conditions, such as initial P

concentration and the presence of competitive ions; (ii) evaluate the seeding phenomena and assess its viability for implementation in industrial processes; and (iii) characterize the obtained product in different operating conditions. The results obtained with the synthetic solutions is further expanded using wastewater samples, which is a system with a much higher degree of complexity. The results provided by this work may be a good starting point for creating awareness and giving visibility and credibility to the possibility of implementing this technology in practice on a pilot-scale WWTP.

2. Materials and Methods

2.1. Samples Collection and Analytical Methods

The synthetic solutions were obtained by dissolving sources of P (KH_2PO_4), Mg ($MgCl_2{\cdot}6H_2O$), and N (NH_4Cl) in specific quantities, as indicated in Section 2.3.

Three wastewater samples were gathered from a Portuguese WWTP, with a treatment capacity of about 40,000 m^3/day, which includes activated sludge systems as secondary treatment and anaerobic digestion for sewage sludge management.

One sample was collected before anaerobic digestion (sample WW1), whereas the other two were collected at different times after the dewatering step by centrifugation (samples WW2.1 and WW2.2). The selection of the collection point was based on previous work according to the initial phosphorus concentration needed to precipitate struvite [13,21]. The biomass ash used as the seeding agent was obtained from a biomass thermoelectric plant in the central region of Portugal. Table 1 summarizes the main characteristics of the wastewater samples and biomass ash (with a particle size < 250 μm).

Table 1. Characterization of wastewater and biomass ash samples.

	Wastewater Samples			**Solid Sample**
Parameter	WW1	WW2.1	WW2.2	Biomass ash (pd < 250 μm)
TS (%)	2.03 ± 0.04	0.41 ± 0.02	1.66 ± 0.01	98.9 ± 0.10
		(mg/L)		(g/kg)
TKN	1128 ± 18	1025 ± 65	994 ± 14	-
TP	496 ± 53	325 ± 12	121 ± 1.04	0.75 ± 0.17
sTP	410 ± 15	205 ± 1.21	90.2 ± 0.69	-
tRP	339 ± 2.48	144 ± 4.13	118 ± 8.32	-
sRP	129 ± 6.12	77 ± 1.02	41 ± 0.38	-
Mg	136 ± 0.22	112 ± 0.80	101 ± 0.92	19.0 ± 1.20
Ca	191 ± 0.56	204 ± 1.24	224 ± 0.42	195 ± 18
Na	91.7 ± 0.08	84.6 ± 0.01	107 ± 0.03	-
K	36.3 ± 1.58	29.7 ± 0.36	35.5 ± 0.21	23.3 ± 2.83
Mg/P molar ratio *	1.34	1.85	3.13	-
Ca/P molar ratio *	1.14	2.05	4.22	-
EC (mS/cm)	9.01	8.58	9.08	12.5
pH	5.46	7.13	6.95	12.8

WW1—sample before anaerobic digestion; WW2.1 and WW2.2—samples after anaerobic digestion and dewatering with centrifugation; pd—particle diameter; EC—electrical conductivity; TS—total solids; TP—total phosphorus; sTP—soluble total phosphorus; tRP—total reactive phosphorus; sRP—soluble reactive phosphorus (orthophosphates); * Mg/P and Ca/P molar ratio were calculated regarding the sRP; potentially toxic metals in biomass ash (mg/kg): Cr—19.8 ± 4.0; Ni—26.7 ± 3.4; Cu—39.2 ± 5.9; Zn—128.3 ± 8.6; Pb—49.3 ± 6.9.

The pH and electrical conductivity (EC) were measured in the liquid with a Consort C1020 instrument. Total solids (TS) and P content determination followed EPA Methods 1684 and 365.3 (ascorbic acid method using a spectrophotometer at 650 nm), respectively. Total P (TP) and soluble TP (sTP) were determined by colorimetry after digestion with persulfate in the sample without, and with, filtration (0.45 μm filter), respectively. Total reactive P (tRP) and soluble reactive P (sRP—orthophosphates) were obtained directly by colorimetry without, and with, filtration (0.45 μm filter), respectively. The K, Mg, Ca, and Na concentrations were obtained through flame atomic absorption spectroscopy (Analytik

Jena ContrAA 300, Jena, Germany). In the case of biomass ash, before P, Mg, and Ca determination, acid digestion with aqua regia was required. Nitrogen concentration was determined according to the Kjeldahl method.

2.2. Precipitation Experiments: Synthetic and Wastewater Solutions

Figure 1 illustrates the experimental setup: Step 1—wastewater preparation; Step 2—precipitation process; and Step 3—analysis of the supernatant and the precipitate. Step 1 was applied only to the wastewater experiments. For the synthetic solutions, only steps 2 and 3 were required.

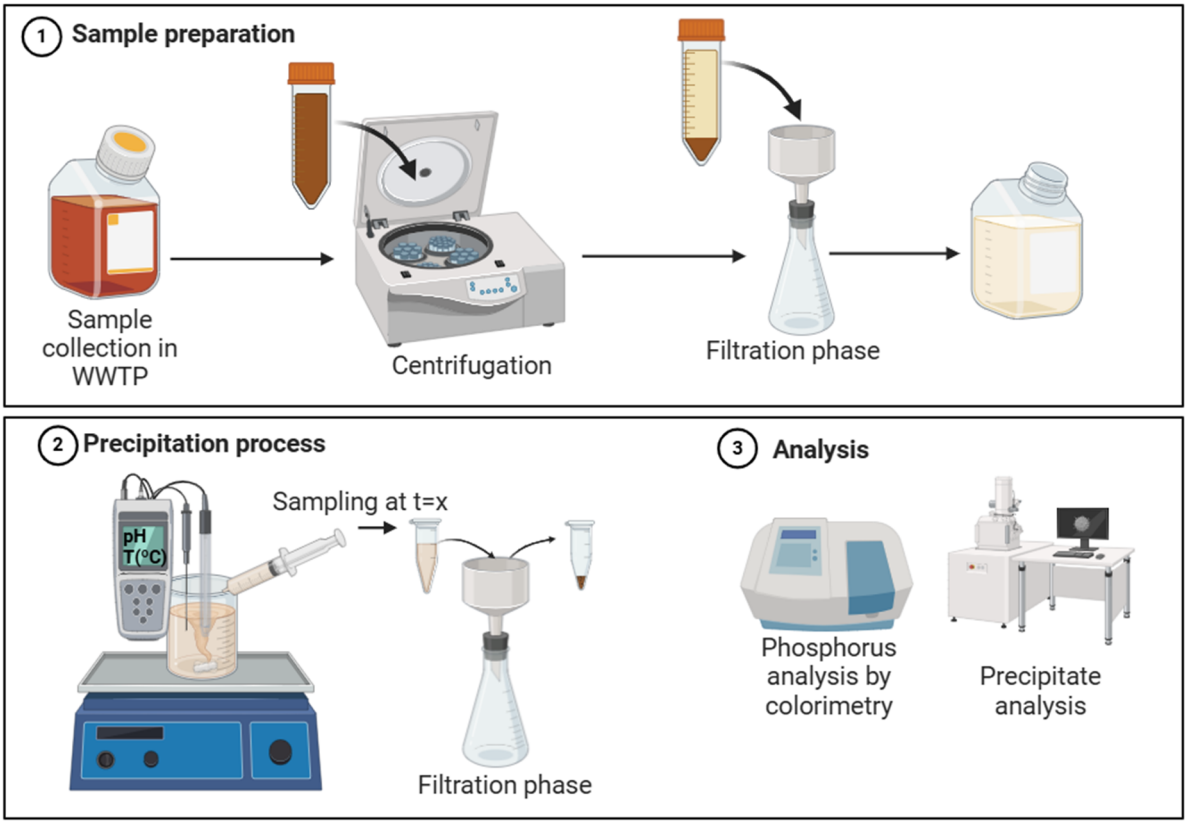

Figure 1. Experimental setup with real wastewater (steps 1–3) and synthetic solutions (steps 2 and 3).

Initially, the experiments with synthetic solutions were based on mixtures of P (KH_2PO_4), Mg ($MgCl_2 \cdot 6H_2O$), and N (NH_4Cl) in equal molar ratios. The precipitation experiments were carried out with 500 mL of solution under magnetic agitation (100 rpm), maintaining the pH at 9 (NaOH, 1 M) and the temperature (20 ± 1 °C, room temperature) constant. Samples were collected at pre-determined times, filtered with a 0.45 µm pore filter, and the supernatant was analyzed to determine P content. The removal efficiency of P, $R_{Ef,P}$ (%), was obtained by Equation (2), considering the soluble reactive phosphorus, as follows:

$$R_{Ef,P}(\%) = \left(1 - \frac{C_{t,P}}{C_{0,P}}\right) \cdot 100 \quad (2)$$

where $C_{t,P}$ and $C_{0,P}$ are the concentrations (mg P/L) at time t and the initial instant, respectively.

The reaction kinetics was modeled assuming a first-order kinetic model, according to Equation (3), as follows:

$$\frac{dC}{dt} = -k(C_{t,P} - C_{eq,P}) \quad (3)$$

where k (1/min) is the kinetic constant, $C_{t,P}$ (mg P/L) is the concentration of P at time t, and $C_{eq,P}$ (mg P/L) is the concentration of P at equilibrium time. By integrating Equation (3),

with the initial condition, $C_{t,P}$ (t = 0) = $C_{0,P}$, Equation (4) can be obtained after linearization, which was the equation used to determine the kinetic constant (k), as follows:

$$\ln\left(C_{t,P} - C_{eq,P}\right) = -kt + \ln\left(C_{0,P} - C_{eq,P}\right) \quad (4)$$

Moreover, the principal operating parameters were studied to evaluate their impact on P removal efficiency and struvite production. In particular, the influence of the initial P concentration (for a fixed Mg/P of 1) was considered using solutions with 20, 30, 50, 80, and 100 mg P/L. Samples were collected at different times from 0 to 120 min to determine the equilibrium time. The influence of Mg/P was determined for 0.5, 1, and 2 by fixing the initial P concentration at 100 mg P/L and a reaction time of 60 min (fixed after equilibrium tests). The impact of temperature was evaluated considering the range with relevance to real WWTP. In particular, 20 °C (room temperature), 30 °C, and 40 °C were tested for a fixed Mg/P of 1 and a concentration of 100 mg P/L.

The impact of coexisting ions on P removal efficiency (initial conditions: 100 mg P/L, Mg/P 1) was studied for two main ions present in wastewater, Ca^{2+} and Na^{+}, which are potential interferences. The estimated range of concentrations found in wastewater for these two ions is 10–150 mg/L for Ca^{2+} and 40–400 mg/L for Na^{+} [22]. Thus, the Ca^{2+} influence was tested for 50, 100, and 200 mg/L using $CaCl_2$, whereas the Na^{+} impact was evaluated at concentrations of 100, 250, 500, and 10,700 mg/L using pure NaCl. The highest Na concentration was used to simulate the concentrations present in the seawater; a common low-cost source of Mg studied in the literature, as a substitute for commercial Mg sources (e.g., $MgCl_2 \cdot 6H_2O$, $MgSO_4 \cdot 7H_2O$) [23,24].

The seeding effect on crystallization was studied using struvite (previously prepared) and biomass ash particles. In these tests, the initial conditions were 100 mg P/L and Mg/P 1. Struvite crystals were produced in synthetic solutions with 100 mg P/L and an Mg/P 1. For struvite seeds, the sizes tested were 38–63 µm and 63–250 µm, whereas for biomass ash, the sample was sieved for sizes < 63 µm and 63–250 µm. The load of the seed was 0.5 g/L [25–29].

To carry out the tests with wastewater, the samples collected were centrifugated for 10 min, and then filtrated to remove gross suspended solids (Figure 1—step 1). The filtered wastewaters were used to produce struvite at a pH of 9 (adjusted with NaOH), using a Mg/P 1, and at room temperature (20 ± 1 °C).

2.3. Precipitation Characterization

The precipitate morphology and elements distribution were obtained by scanning electron microscopy coupled with energy dispersive X-ray spectrometry (SEM-EDS, SU-70 SEM Hitachi (Tokyo, Japan), and Quantax 400 Bruker EDS (Billerica, MA, USA)). X-ray diffraction (XRD, PANalytical XPert PRO diffractometer, with CuKα radiation; Malvern Panalytical, Malvern, UK) and Panalytical HighScore Plus 4.7 (PDF-4) software were used to determine the crystalline phases of the materials.

2.4. Chemical Equilibrium Simulations and Statistical Analysis

Visual MINTEQ chemical equilibrium software (version 4.05) was used to calculate the saturation indices (SI) and mass distribution between dissolved species and solid phases. This tool helped in results interpretation for the comparison of real and theoretical scenarios. The results express the ionic activity, and if the product of activities is greater than K_{sp} (between $10^{-12.6}$ and $10^{-13.26}$ [11]), then SI > 0, the solution is supersaturated and precipitation will occur.

A one-way ANOVA was used to evaluate statistical differences between the parameters analyzed using Astatsa online software (https://astatsa.com/). If significant differences were found ($p < 0.05$) pairwise comparisons were carried out to identify the statistically significant differences using the post hoc Tukey HSD test ($p < 0.05$).

3. Results and Discussion

3.1. Influence of the Main Operating Conditions

As aforementioned, the struvite precipitation depends on several operating variables, but pH, initial concentration of P, Mg/P molar ratio, and temperature were considered the main ones.

According to the literature, the concentration (and speciation) of Mg^{2+}, NH_4^+, and PO_4^{3-} is controlled by pH. Based on speciation curves in pure water, the optimum pH range for promoting struvite formation is between 8 and 11, as the concentrations of NH_4^+ and PO_4^{3-} are the highest possible [17]. In addition, the pH also affects the formation of other precipitates relevant to the system under analysis, such as $MgHPO_4{\cdot}3H_2O$ [17]. According to the literature and the experiments conducted in the present study (Figure S1, Supplementary Materials), the highest removal efficiency (near 80%) was observed at a pH of 9. Therefore, this pH value was set to carry out the following tests [30,31].

The P concentration in wastewater can vary within a wide range of values and, along with the Mg/P molar ratio, is a variable that influences the P removal efficiency by struvite precipitation. Thus, it is important to investigate the minimum initial P and Mg concentrations required to promote an efficient process (removal efficiency > 60% [12]). These assays were carried out with synthetic solutions, and according to Figure 2, negligible P recoveries were observed for concentrations below 30 mg P/L. Indeed, only 4% of P was recovered from a solution with an initial concentration of 20 mg P/L. Additionally, in the Visual MINTEQ prediction at the same pH and temperature conditions, the Saturation Index (SI) of struvite was negative (−0.190) for 20 mg P/L, showing no potential formation of this mineral. However, for 30 mg P/L the SI was already positive (0.249). Moreover, through Visual MINTEQ simulations, various minerals in the analyzed system may be formed, but only those with the highest potential for precipitation are summarized in Table 2. In fact, some minerals are likely to precipitate in specific conditions since they are associated with SI > 0, whereas those that remain dissolved in solution have a negative SI. Thus, there was a decrease in SI for all species ($Mg_3(PO_4)_2$, $MgHPO_4{\cdot}3H_2O$, and struvite) as the initial concentration of P decreased. Thus, this fact supports the results that RP decreased as the initial concentration of P in the solution also decreased.

Table 2. Prediction of Visual MINTEQ for minerals formed and respective saturation index for different P initial concentrations.

	Saturation Index of Minerals		
$C_{0,P}$ (mg P/L)	$Mg_3(PO_4)_2$	$MgHPO_4{\cdot}3H_2O$	Struvite
100	2.053	0.009	1.480
80	1.739	−0.118	1.260
50	1.043	−0.396	0.784
30	0.247	−0.714	0.249
20	−8.159	−0.419	−0.190
10	−9.294	−1.625	−0.968

$C_{0,P}$—initial phosphorus concentration.

Figure 3 shows the results for different Mg/P molar ratios, where the removal efficiency is superior for the highest value, as expected. For Mg/P 2, the amount of Mg is stoichiometrically higher than required to form struvite, promoting the P recovery by other complexes. For example, $Mg_3(PO_4)_2$ has an inferior solubility product constant ($10^{-25.2}$ [32]) compared to struvite (with the most reported values between $10^{-12.6}$ and $10^{-13.26}$ [17]), showing the potential to co-precipitate and form impurities in the final product (struvite). Indeed, other authors report the negative impact of higher Mg/P molar ratios in struvite purity [30].

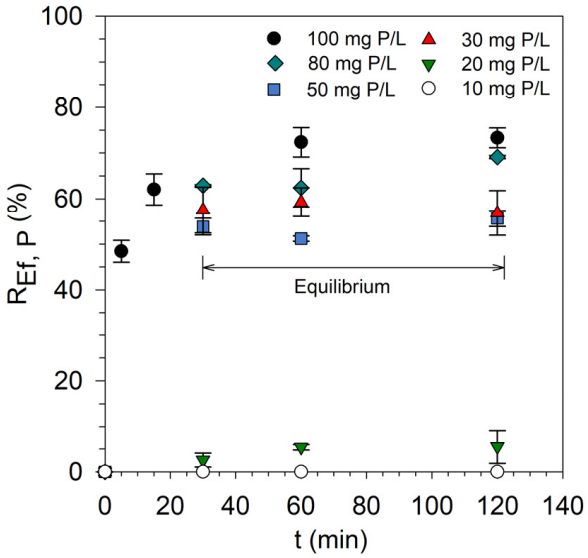

Figure 2. Influence of phosphorus initial concentration (at Mg/P molar ratio 1) on removal efficiency for synthetic solutions [pH 9, 20 ± 1 °C].

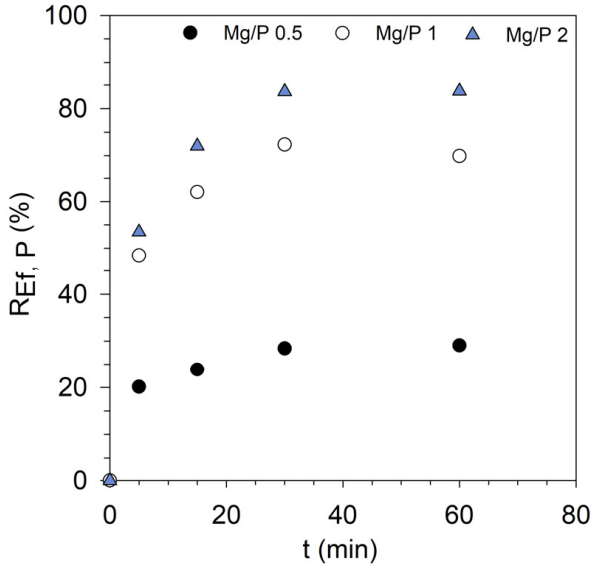

Figure 3. Influence of Mg/P molar ratio (100 mg P/L initial concentration) on removal efficiency for synthetic solutions [pH 9, 20 ± 1 °C].

As shown in Figure 3, the time for recovery of the same amount of P is reduced for higher Mg/P molar ratios. After 60 min of reaction, it was possible to remove about 70 and 80% of the P present in the solution for Mg/P 1 and 2, respectively. Even though a wide range of values was analyzed in this study, wastewater composition can be quite variable; thus, the Mg/P can also vary significantly. These results led to the conclusion that, with an Mg/P above 1, the process is potentially viable (removal efficiency > 60%). Considering the importance of obtaining the purest struvite product possible (better fertilizer behavior and market selling cost), a compromise between the removal efficiency and the purity of the material should be made. Thus, considering the predictions of Visual MINTEQ in Table 3, Mg/P 1 provided a better response for both parameters.

When considering the real application scenario of struvite recovery after anaerobic digestion in the WWTP, which normally operates between 30 and 40 °C, it is important to verify whether temperature influences the formation of struvite. Figure 4 and Table 4 show that the removal efficiencies and final concentrations of P at 60 min of reaction were similar

at all three temperatures. At 40 °C, the kinetic constant is superior (0.336 min^{-1}), indicating that the reaction occurs more rapidly, but the final $R_{Ef,P}$ and $C_{eq,P}$ are statistically equal to the other temperatures. Therefore, it can be concluded that implementing the phosphorus recovery method using struvite after anaerobic digestion is favorable, as the temperature does not inhibit its removal.

Table 3. Prediction of Visual MINTEQ for potential minerals formed and respective saturation index for different initial Mg/P molar ratios.

Mg/P Molar Ratio	Saturation Index of Minerals		
	$Mg_3(PO_4)_2$	$MgHPO_4 \cdot 3H_2O$	Struvite
0.5	1.423	−0.124	1.453
1	2.053	0.009	1.480
2	3.151	0.513	1.974

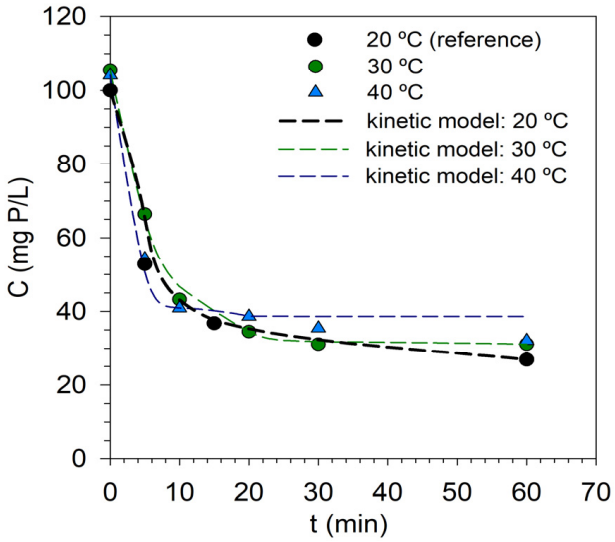

Figure 4. Experimental data and prediction of the reaction kinetic model at different temperatures [pH 9, Mg/P molar ratio 1, 100 mg P/L].

Table 4. Kinetic reaction constant and P recovery values for different temperatures.

T (°C)	k (1/min) *	$R_{Ef,P}$ (%)	$C_{eq,P}$ (mg P/L)
20	0.079	69.9 ± 1.8	31.0 ± 1.9
30	0.156	70.5 ± 0.3	31.1 ± 2.3
40	0.336	62.9 ± 0.1	38.6 ± 0.1

k—kinetic constant; $R_{Ef,P}$—phosphorus removal efficiency after 60 min; $C_{eq,P}$—phosphorus equilibrium concentration after 60 min; * Figure S2—Supplementary Materials.

Based on the previous results, the ideal conditions to carry out the following tests were chosen: an initial concentration of 100 mg P/L, Mg/P 1, and a temperature of 20 °C. The XRD analysis showed that the solid precipitated in these conditions has a principal crystalline phase of struvite (92%wt), and a second phase of $MgHPO_4 \cdot 3H_2O$ (8%wt) (Figure S3, Supplementary Materials).

3.2. Influence of Coexisting Ions

The effects of the two ions commonly present in wastewater (calcium and sodium) were studied, as shown in Figures 5 and 6. Calcium has a significant influence on the initiation of the P removal reaction. Indeed, the P removal efficiencies, $R_{Ef,P}$, for the different Ca concentrations tested, in the first 5 min of the reaction, were statistically different from that of the blank solution (0 mg Ca/L) (Figure 5b, bars marked with different letters).

The kinetic constant increased from 0.0791 min^{-1} to 0.1074 and 0.1699 min^{-1} (Figure S4, Supplementary Materials) for 0, 50, and 100 mg Ca/L, respectively, indicating that the removal of P was faster as the Ca concentration increased. However, after 60 min of reaction, the final removal efficiencies were similar for 0, 50, and 100 mg Ca/L, with values of 69, 73, and 77%, respectively. Nonetheless, in the case of adding 200 mg Ca/L, not only was the reaction the fastest (kinetic constant of 0.7355 min^{-1}; Figure S4—Supplementary Materials), but the $R_{Ef,P}$ was also greater than 80% in the first 5 min. In this case, the removal efficiency at 60 min increased by more than 20% compared to the blank (0 mg Ca/L).

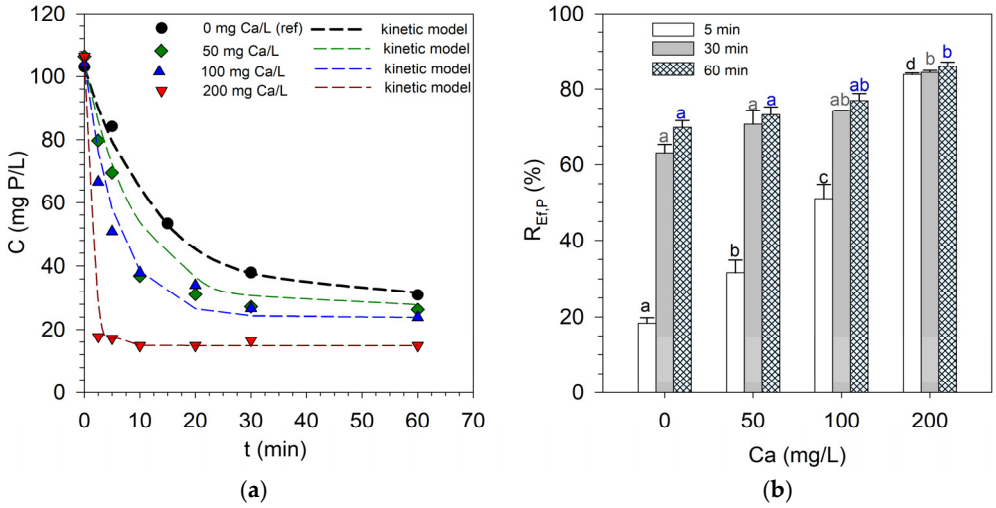

Figure 5. (**a**) Experimental data and prediction of the reaction kinetic model for different calcium concentrations; and (**b**) influence of calcium concentrations on removal efficiency [different letters mean statistically different results for $p < 0.05$; statistical analysis was performed for each reaction time: 0, 30 and 60 min; pH 9; 100 mg P/L, 20 ± 1 °C, Mg/P molar ratio 1].

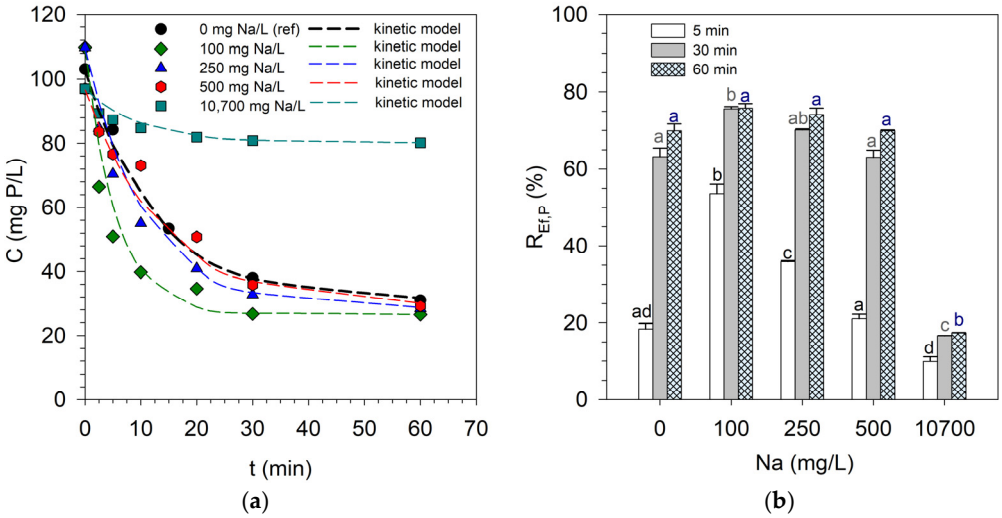

Figure 6. (**a**) Experimental data and prediction of the reaction kinetic model for different sodium concentrations; and (**b**) influence of sodium concentrations on removal efficiency [different letters mean statistically different results for $p < 0.05$; statistical analysis was performed for each reaction time separately; pH 9; 100 mg P/L, 20 ± 1 °C; Mg/P molar ratio 1].

According to the Visual MINTEQ predictions (Table 5), as the concentration of Ca increased from 0 to 200 mg/L, the SI of struvite decreased, while the SI of hydroxyapatite and the other minerals increased. Other researchers, who reported that a higher concentration of Ca in the system enhances the formation of hydroxyapatite, corroborate the results of the present study. Struvite and hydroxyapatite are likely to form when the Mg/Ca molar

ratio is 2. In contrast, when the Mg/Ca molar ratio is 0.5, only hydroxyapatite is expected to form [18]. Indeed, XRD analysis of the precipitates formed at 100 revealed that the solid formed contained struvite as the only crystalline phase (Figure S5, Supplementary Materials). On the other hand, the precipitate formed at 200 mg Ca/L was amorphous, suggesting the possibility of the formation of non-crystalline calcium phosphates. Similar results were found in a study developed by Campos et al. (2023), where the XRD patterns of solids obtained in the presence of calcium reveal low-intensity peaks of struvite and the possible formation of amorphous calcium phosphate as a coprecipitated material [33]. Another study detected two phosphorus crystalline phases in synthetic solutions containing Mg, P, N, and Ca: struvite and hydroxyapatite [34]. These authors concluded that the intensity of struvite peaks decreased as the Mg/Ca molar ratio decreases. The sample precipitated in a solution with a Ca content twice as high as Mg proved to be quite amorphous, with only hydroxyapatite being identified in the sample, indicating complete inhibition of struvite precipitation [34]. New alternatives should be explored in further work to avoid the "contamination" of the sample with calcium, and the literature suggests an increase in the Mg/Ca molar ratio or selective calcium removal [35,36].

Table 5. Predictions of Visual MINTEQ for potential minerals formed and respective saturation index for different calcium and sodium concentrations [pH 9, 100 mg P/L, 20 ± 1 °C, Mg/P molar ratio 1].

	Saturation Index							
	$C_{0,Ca}$ (mg/L)				**$C_{0,Na}$ (mg/L)**			
Mineral	0	50	100	200	100	250	500	10,700
$Mg_3(PO_4)_2$	2.053				2.261	2.193	2.088	−0.334
$MgHPO_4 \cdot 3H_2O$	0.009				0.41	0.206	0.154	−0.994
Struvite	1.480	1.289	1.204	1.046	1.700	1.660	1.602	0.416
$Ca_3(PO_4)_2$		5.804	6.634	7.361				
$CaHPO_4$		0.443	0.686	0.872				
Hydroxyapatite		16.932	18.351	19.618				
$Mg_3(PO_4)_2$		1.289	1.204	1.046				

$C_{0,Ca}$—initial calcium concentration; $C_{0,Na}$—initial sodium concentration.

Regarding the presence of Na in the solutions, Figure 6a,b demonstrates that, from 100 to 500 mg Na/L, the impact on the P removal efficiency was not statistically relevant ($p < 0.05$). The same is not true for the concentration of 10,700 mg Na/L, where a significant inhibition of the P removal was observed ($R_{Ef,P} \leq 20\%$). Therefore, it is concluded that replacing the Mg source with seawater is not viable, since Na in high concentrations makes P removal difficult. In the literature, there are some studies where seawater is suggested as a source of Mg [24,37,38]. However, other authors stated that seawater tends to form several complexes due to the presence of large quantities of Na^+ and Ca^{2+} ions, thus reducing struvite purity compared to tests with $MgCl_2$ [39]. At a concentration of 10,700 mg Na/L, Table 5 shows that there was a significant reduction in the SI of struvite and $Mg_3(PO_4)_2$, which supports the lower P removal efficiencies.

The literature corroborates these results, indicating that Na^+ concentrations above 1150 mg/L increase the induction time for crystal formation. Despite the increase in supersaturation of the solution, the induction time may rise due to the accumulation of positive charges of Na^+ around molecules with negative charges, such as struvite, hindering the nucleation process [40]. In addition, Kabdasli et al. (2018) explained that this increase in Na^+ charges on the surface of the nuclei forms a barrier that slows down the transport of Mg^{2+} and NH_4^+ to them [41].

3.3. Influence of Seeding

Two types of seeds were tested to evaluate the influence of this phenomenon, struvite (inducing secondary nucleation) and biomass ash (primary nucleation). Figure 7 and

Table 6 highlight the results obtained. The present results refer to the first 10 min because it is in the initial reaction period that the seeds can act to accelerate the process.

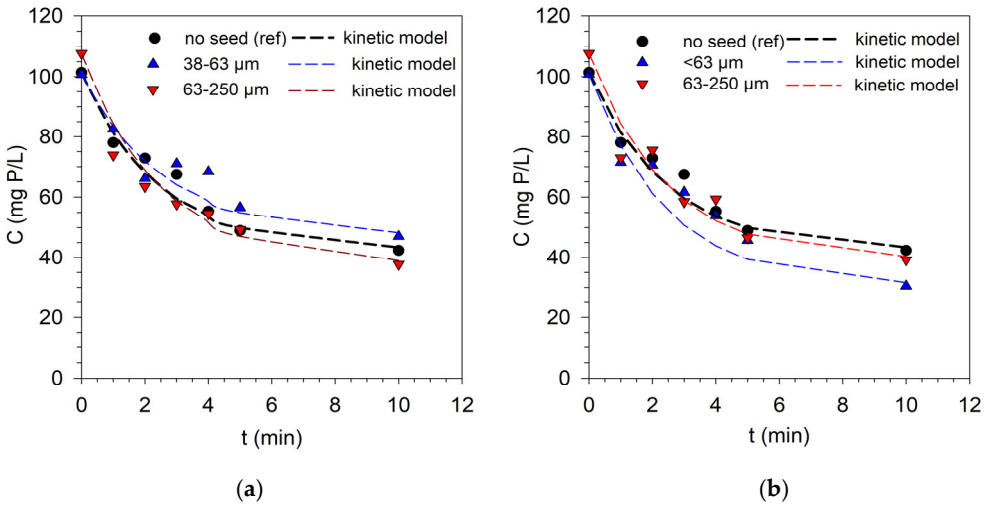

Figure 7. Decrease in P concentration in the first 10 min of reaction using different seeds sizes: (**a**) struvite; and (**b**) biomass ash [pH 9, 100 mg P/L, 20 ± 1 °C, Mg/P molar ratio 1, load of seed = 0.5 g/L].

Table 6. Kinetic reaction constants and P recovery values (t = 10 min) for different seed types.

Seed Type	Seed Size (µm)	k (1/min) *	$R_{Ef,P}$ (%)	C (mg P/L)
No seed	-	0.413	58.2 ± 0.32	42.3 ± 0.33
Struvite	38–63	0.385	53.3 ± 1.22	47.1 ± 0.51
	63–250	0.403	64.8 ± 4.11	37.6 ± 1.96
Biomass ash	<63	0.416	69.8 ± 5.67	30.5 ± 5.81
	63–250	0.410	63.6 ± 0.56	39.2 ± 0.62

k—kinetic constant; $R_{Ef,P}$—phosphorus removal efficiency after 10 min; C—phosphorus concentration at 10 min reaction time; * Figure S6—Supplementary Materials.

As can be seen in Figure 7 and Table 6, the kinetic constants are similar for all the experiments without and with seeds of different types and sizes. The P removal efficiencies after 10 min were statistically equal between the experiments without and with seeds of struvite ($p < 0.05$). Although seeding is expected to boost nucleation efficacy and reduce induction time by increasing reaction surface area [25], other studies also found no evident differences when seeding with struvite compared to the identical reaction without seeding [27]. The reason for this could be that the reaction reaches equilibrium quickly, and the newly created crystal nuclei have a larger surface area than the seeds introduced into the system [27]. Regardless, the use of struvite seeds presents an advantage in that the surface for nucleation is the same as that which will be formed, resulting in a uniform product. In addition, the use of struvite minimizes the contamination of the system with other impurities.

Using biomass ash, seeds smaller than 63 µm had the maximum removal effectiveness (almost 70%). This enhancement could be attributed to the fact that the surface area of the seeds is similar to the surface of the new struvite nuclei generated, promoting the development of this mineral on the surface of the seeds and allowing very small nuclei to form on these surfaces without being lost [1]. Another crucial factor verified with the biomass ash seeds was an increase in the initial pH of the solution from 4.6 to 7.2. Despite these tests being developed in synthetic solutions, this increase in pH allows for a reduction in the use of a pH control solution (e.g., NaOH), reducing the costs in real-scale processes. Other studies in the literature use alternative sources for seeding such as biochar. A study from the literature carried out experiments with two types of biochar, obtaining a 43% increase in crystal size when compared to the process without seeding. These authors also

reported that the crystal formed with biochar seeding had an internal crystalline structure similar to the struvite produced without seeding. However, there was also an increase in heavy metals concentrations, which is a disadvantage to this product for applications in the soil. In addition, the study showed that there is no beneficial effect in increasing the amount of seed from 0.75 to 1 g/L [26]. A study conducted by other authors also disclosed an increase in P removal efficiency from 88 to 97% (biochar seed) and 95% (struvite seed) compared to the process without seeding [42]. Thus, these alternative seeding sources could be an asset to enhance the process.

The precipitate obtained in the presence of biomass ash seeds (size < 63 μm) was investigated by XRD to determine the level of impurities in the final product. The principal crystalline phase determined was struvite (about 68%wt), while P was also removed as $(Mg_3Ca_3PO_4)_4$. The XRD also found quartz (11%wt) and calcium carbonate (18%wt) phases, which was expected given that biomass ash contains silica, carbonates, and calcium (Figure S7, Supplementary Materials).

Figure 8 presents SEM images with the precipitate obtained without, and with, biomass seeds (size < 63 μm). There are some differences between the samples due to the presence of compounds with silica, calcium, and carbonates, as is shown in Figure 8b,d. However, in both images, the presence of struvite (crystals with more elongated form) can be observed.

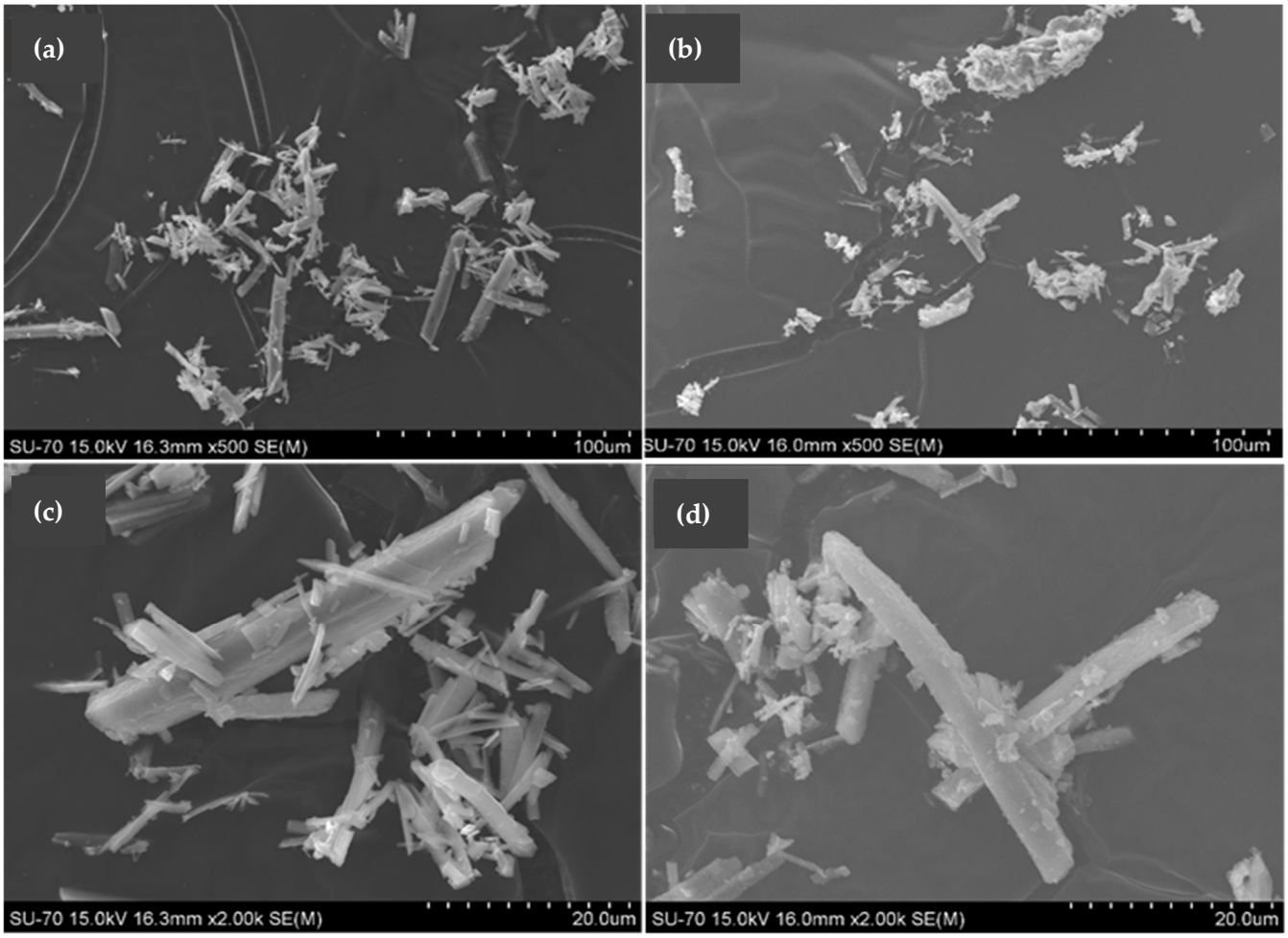

Figure 8. SEM images of precipitated solid: (**a**) solid without seed—pH 9, 100 mg P/L, 20 ± 1 °C, Mg/P molar ratio 1, with magnification 500×; (**b**) solid with biomass ash seeds (<63 μm) with magnification 500×; (**c**) solid without seed—pH 9, 100 mg P/L, 20 ± 1 °C, Mg/P molar ratio 1, with magnification 2000×; (**d**) solid with biomass ash seeds (<63 μm) with magnification 2000×.

Out of the 22 crystals that were examined, and are shown Figure 8a, the length found was between 9.5 and 48.4 µm, while four had larger diameters, from 39 to 48.4 µm. Regarding the crystals obtained with biomass ash seeds, the size range was between 6.6 and 40 µm.

A complementary mapping analysis was conducted. Figure S8 (Supplementary Materials) shows that, across the elongated shape of the struvite crystal in both precipitate samples, other elements were identified. Mg, N, and P are primarily grouped in the crystal area (more intense color), confirming that it corresponds to struvite. The Ca appeared when biomass ash was used for seeding, although it was dispersed over the whole sampling area. This suggests that the Ca mineral surrounding the struvite crystal may be related to calcium carbonate and/or $(Mg_3Ca_3PO_4)_4$.

3.4. Precipitation with Wastewater

As highlighted in the results shown in Table 7, the P removal efficiencies surpassed the expected and predicted values in the analyses of the synthetic solutions. Furthermore, the recoveries obtained were not significantly influenced by the point in WWTP at which the samples were collected. Removal efficiencies of 95% [22] and 93.2% [15] were also found in the literature for Mg/P molar ratios of 1 and 2.5 in wastewater matrices. According to the XRD analyses of sample S2.2, struvite represented only 15%wt of the solid, while hazenite ($KNaMg_2(PO_4)_2 \cdot 14H_2O$) was about 23%wt. In this case, the main crystalline phase detected was halite (NaCl), representing about 62% of the solid (Figure S9, Supplementary Materials). This result may be due to the high concentration of sodium and chloride present in the sample, as the WWTP is located near the sea. In these cases, the precipitate of struvite should be previously washed to avoid contamination before its application in soil.

Table 7. P removal values and equilibrium concentrations for the different wastewater samples after 60 min of reaction.

Sample	$C_{0,P}$ (mg P/L)	$R_{Ef,P}$ (%)	$C_{eq,P}$ (mg P/L)
WW1	129	94.5 ± 0.18	7.10 ± 0.24
WW2.1	77	91.6 ± 0.19	6.48 ± 0.15
WW2.2	41	89.9 ± 0.36	4.14 ± 0.15

$C_{0,P}$—initial phosphorus concentration in terms of soluble reactive phosphorus (orthophosphate); $R_{Ef,P}$—phosphorus removal efficiency after 60 min; $C_{eq,P}$—phosphorus equilibrium concentration at 60 min.

The results in the present study showed that P removal was mainly due to the formation of two minerals, hazenite, and struvite (in lower mass percentage). In the literature, several studies report two compounds derived from struvite, struvite-Na ($NaMgPO_4 \cdot 7H_2O$) and struvite-K ($KMgPO_4 \cdot 6H_2O$). The formation of these compounds tends to occur when sodium and potassium are in excess in the matrix; in both cases, the ions Na^+ or K^+ substitute the NH_4^+ [43,44]. Furthermore, the solubility product of struvite is between $10^{-12.6}$ and $10^{-13.26}$ [9], that of struvite-K is $10^{-10.62}$ [45] and that of struvite-Na is $10^{-11.6}$ [46]. Another study addressing hazenite formation stated that this mineral is similar to struvite. The study demonstrated that P composition in hazenite is about 11.2%, while that in struvite is 12.6% [47]. Therefore, hazenite may have fertilization interest, and like struvite, the compound may have low solubility in water, acting as a slow-release fertilizer.

According to the Visual MINTEQ predictions, the mineral with the highest probability of precipitating in wastewater conditions was hydroxyapatite, with an SI of 16.970, compared to that of 1.408 for struvite, mainly due to the calcium concentration in the matrix. However, no calcium mineral was detected in the XRD analyses, which indicates that calcium probably precipitated in the amorphous phases. Regarding struvite-K, and struvite-Na, or the combination of both (hazenite), there were also no predictions for their formation. These differences between the real and synthetic solutions result from the fact that the former effluent contains many elements and organic matter that determine the

complex equilibrium between the phases that precipitate and the substances that remain in the solution.

SEM analysis was carried out for the precipitate from the WW2.2 sample. Figure 9a,c shows the images obtained for the synthetic solution, while Figure 9b,d shows the images for the real sample. Differences are easily detected, as the images in Figure 9a,c depict well-defined struvite crystals, whereas Figure 9b,c shows not only struvite crystals (corresponding to more elongated structures) but also other clusters of particles nearby the crystals, making their identification difficult. Some of the clusters next to the struvite are probably halite, as it is the compound that represents most of the solid precipitate sample.

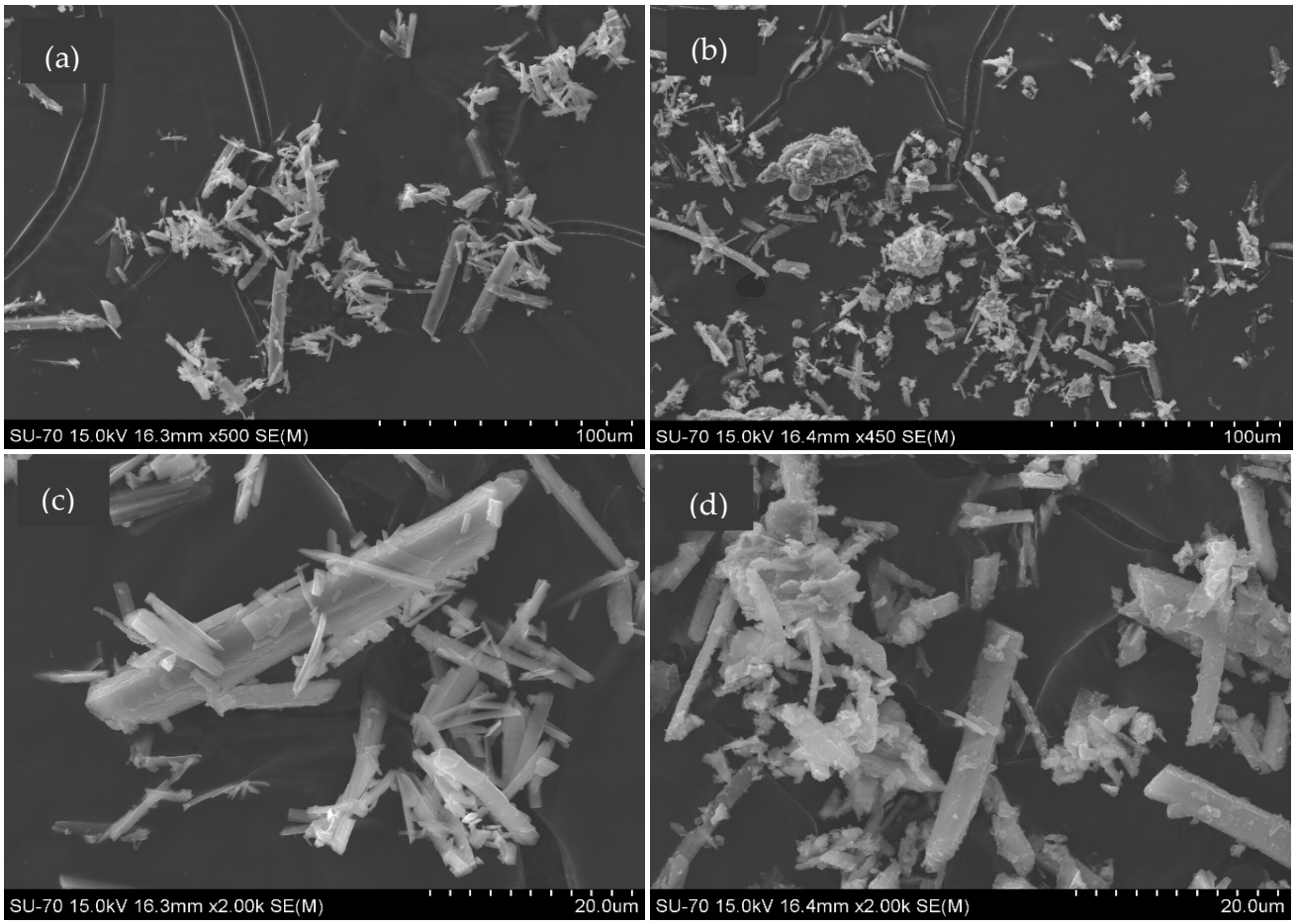

Figure 9. SEM images of precipitated solid: (**a**) synthetic solution—pH 9, 100 mg P/L, 20 ± 1 °C, Mg/P 1, with magnification 500×; (**b**) WW2.2. wastewater sample with magnification 500×; (**c**) synthetic solution—pH 9, 100 mg P/L, 20 ± 1 °C, Mg/P 1, with magnification 2000×; and (**d**) S2.2. wastewater sample with magnification 2000×.

4. Conclusions

This work focused on the main variables that influence phosphorus removal from liquid matrices as struvite for future application in a wastewater treatment scenario. The first assessment revealed that the minimal P concentration required to promote struvite precipitation was 30 mg P/L. However, removal efficiencies were, approximately, 50% in this case (not economically viable). The studies with an Mg/P 2 demonstrated higher removal efficiencies than those with an Mg/P 1, ranging from 70% to more than 80%. However, given the economic costs of additional Mg sources, this ratio will not be favorable and may result in more impurities in the final product. An alternative is exploring the use of different magnesium sources, namely byproducts with low commercial value. Nevertheless, this ratio may be valid if the wastewater already contains these P and Mg concentrations.

According to the analysis of coexisting ions, results indicate that calcium has a significant influence on P removal as pure struvite. The removal efficiency of P was about 86% for calcium concentrations of 200 mg P/L, compared to around 70% when no calcium was present. Indeed, the XRD analysis revealed that the resulting precipitate was amorphous. Thus, calcium will have a notorious impact on struvite purity, and in future work, this issue must be explored.

The seeding experiments showed that struvite seeds did not boost nucleation efficiency. On the contrary, seeds with biomass ash (size < 63 μm) improved the removal efficiency compared to the sample without the seed. It is relevant to note that the wastewater showed a very high buffering capacity, requiring a large amount of base (NaOH) to control the pH at 9 over the experiments. Therefore, the use of biomass ash as a seed agent may be favorable to this process. As previously mentioned, the biomass ash helped in the increase of the initial pH of the solution, and thus reduced the required NaOH to adjust the pH (lower operating process costs). Although the recoveries of P in the real context seemed relatively high, the use of biomass ash may be helpful regarding pH control, and this should be explored in further work. To conclude, some experiments with wastewater were carried out, demonstrating that, despite the good P removal efficiencies (above 90%), the XRD analyses identified struvite as a minority phase (15%wt).

One of the relevant conclusions provided by this work is that the future of the wastewater treatment sector is to explore ways to recover useful compounds during the treatment steps, transforming WWTP into "resource factories". Thus, this study is a starting point for developing a strategy capable of providing an alternative source of fertilizers (struvite), especially in Portugal, where no similar technology is implemented in wastewater treatment systems. However, further work needs to be developed to give credibility to the possibility of implementing this technology in practice, such as: (i) carrying out more extensive tests in wastewater from different collection points, and possibly, at different WWTPs, to assess the variability of the process and (ii) optimizing the process performance in wastewater, mainly focusing on improving P recovery and struvite purity.

Supplementary Materials: The following supporting information can be downloaded at: https://www.mdpi.com/article/10.3390/w16121675/s1, Figure S1. Influence of pH on P removal efficiency [100 mg P/L, Mg/P molar ratio 1, 20 ± 1 °C; different letter means statistically different results ($p < 0.05$)]. Figure S2. Linearization of the kinetic reaction data for different temperatures; Figure S3. XRD spectrum for the precipitate formed in these conditions: initial concentration of 100 mg P/L, Mg/P molar ratio 1, and a temperature of 20 °C; Figure S4. Linearization of the kinetic reaction for different concentrations of (a) calcium and (b) sodium; Figure S5. XRD spectrum for the precipitate formed with 100 mg Ca/L; Figure S6. Linearization of the kinetic reaction data for different seeds size of (a) struvite and (b) biomass ash; Figure S7. XRD spectrum for the precipitate formed in the presence of biomass ash seeds (size < 63 μm); Figure S8. Mapping of different elements in the obtained precipitate (a) without seeds and (b) with seeds of biomass ash (<63 μm); Figure S9. XRD spectrum for the precipitate formed with wastewater.

Author Contributions: Conceptualization, A.F.S., L.S.M. and M.J.Q.; writing-original draft preparation, A.F.S.; writing-review and editing, P.A., L.M.G.-F. and M.J.Q. All authors have read and agreed to the published version of the manuscript.

Funding: Andreia F. Santos acknowledges the Fundação para a Ciência e Tecnologia (FCT) for the Ph.D. Grant (2020.08213.BD). Andreia F. Santos, Luísa S. Mendes, Licínio M. Gando-Ferreira, and Margarida J. Quina acknowledge the financial support to CERES (https://doi.org/10.54499/UIDB/00102/2020, accessed on 4 June 2024), financed by FCT through national funds. P. Alvarenga acknowledges the support of LEAF—Linking Landscape, Environment, Agriculture and Food Research Centre (Ref. UIDB/04129/2020 and UIDP/04129/2020), and the Associate Laboratory TERRA.

Data Availability Statement: No new data were created or analyzed in this study. Data sharing is not applicable to this article.

Conflicts of Interest: The authors declare no conflicts of interest.

References

1. Zhang, T.; Jiang, R.; Deng, Y. Phosphorus Recovery by Struvite Crystallization from Livestock Wastewater and Reuse as Fertilizer: A Review. In *Physico-Chemical Wastewater Treatment and Resource Recovery*; InTech: London, UK, 2017.
2. De Boer, M.A.; Wolzak, L.; Slootweg, J.C. *Phosphorus Recovery and Recycling*, 1st ed.; Ohtake, H., Tsuneda, S., Eds.; Springer: Singapore, 2019; ISBN 978-981-10-8030-2.
3. European Commission. *Study on the Critical Raw Materials for the EU 2023: Final Report*; European Commission: Brussels, Belgium, 2023.
4. Siciliano, A.; Limonti, C.; Curcio, G.M. Advances in Struvite Precipitation Technologies for Nutrients Removal and Recovery from Aqueous Waste and Wastewater. *Sustainability* **2020**, *12*, 7538. [CrossRef]
5. Le Corre, K.S.; Valsami-Jones, E.; Hobbs, P.; Parsons, S.A. Phosphorus recovery from wastewater by struvite crystallization: A review. *Crit. Rev. Environ. Sci. Technol.* **2009**, *39*, 433–477. [CrossRef]
6. Bube, K. Uber Magnesiumammoniumphosphat. *Z. Anal. Chem.* **1910**, *49*, 525–596. [CrossRef]
7. Ohlinger, K.N.; Young, T.M.; Schroeder, E.D. Predicting struvite formation in digestion. *Water Res.* **1998**, *32*, 3607–3614. [CrossRef]
8. Deng, L.; Dhar, B.R. Phosphorus recovery from wastewater via calcium phosphate precipitation: A critical review of methods, progress, and insights. *Chemosphere* **2023**, *330*, 138685. [CrossRef]
9. Talboys, P.J.; Heppell, J.; Roose, T.; Healey, J.R.; Jones, D.L.; Withers, P.J.A. Struvite: A slow-release fertiliser for sustainable phosphorus management? *Plant Soil* **2016**, *401*, 109–123. [CrossRef] [PubMed]
10. Venkiteshwaran, K.; McNamara, P.J.; Mayer, B.K. Meta-analysis of non-reactive phosphorus in water, wastewater, and sludge, and strategies to convert it for enhanced phosphorus removal and recovery. *Sci. Total Environ.* **2018**, *644*, 661–674. [CrossRef]
11. Carrillo, V.; Fuentes, B.; Gómez, G.; Vidal, G. Characterization and recovery of phosphorus from wastewater by combined technologies. *Rev. Environ. Sci. Biotechnol.* **2020**, *19*, 389–418. [CrossRef]
12. Shaddel, S.; Ucar, S.; Andreassen, J.-P.; Østerhus, S.W. Enhancing efficiency and economics of phosphorus recovery process by customizing the product based on sidestream characteristics—An alternative phosphorus recovery strategy. *Water Sci. Technol.* **2019**, *79*, 1777–1789. [CrossRef]
13. Santos, A.F.; Almeida, P.V.; Alvarenga, P.; Gando-Ferreira, L.M.; Quina, M.J. From wastewater to fertilizer products: Alternative paths to mitigate phosphorus demand in European countries. *Chemosphere* **2021**, *284*, 131258. [CrossRef]
14. Shaddel, S.; Ucar, S.; Andreassen, J.-P.; Østerhus, S.W. Engineering of struvite crystals by regulating supersaturation—Correlation with phosphorus recovery, crystal morphology and process efficiency. *J. Environ. Chem. Eng.* **2019**, *7*, 102918. [CrossRef]
15. Krishnamoorthy, N.; Dey, B.; Unpaprom, Y.; Ramaraj, R.; Maniam, G.P.; Govindan, N.; Jayaraman, S.; Arunachalam, T.; Paramasivan, B. Engineering principles and process designs for phosphorus recovery as struvite: A comprehensive review. *J. Environ. Chem. Eng.* **2021**, *9*, 105579. [CrossRef]
16. Li, B.; Huang, H.M.; Boiarkina, I.; Yu, W.; Huang, Y.F.; Wang, G.Q.; Young, B.R. Phosphorus recovery through struvite crystallisation: Recent developments in the understanding of operational factors. *J. Environ. Manag.* **2019**, *248*, 109254. [CrossRef]
17. Tansel, B.; Lunn, G.; Monje, O. Struvite formation and decomposition characteristics for ammonia and phosphorus recovery: A review of magnesium-ammonia-phosphate interactions. *Chemosphere* **2018**, *194*, 504–514. [CrossRef] [PubMed]
18. Acelas, N.Y.; Flórez, E.; López, D. Phosphorus recovery through struvite precipitation from wastewater: Effect of the competitive ions. *Desalin. Water Treat.* **2015**, *54*, 2468–2479. [CrossRef]
19. Zhang, F.; Shan, B.; Wang, Y.; Zhu, Z.; Yu, Z.-Q.; Ma, C.Y. Progress and Opportunities for Utilizing Seeding Techniques in Crystallization Processes. *Org. Process Res. Dev.* **2021**, *25*, 1496–1511. [CrossRef]
20. Myerson, A.S.; Erdemir, D.; Lee, A.Y. (Eds.) *Handbook of Industrial Crystallization*, 3rd ed.; Cambridge University Press: Cambridge, UK, 2019; ISBN 9781139026949.
21. Santos, A.F.; Alvarenga, P.; Gando-Ferreira, L.M.; Quina, M.J. Phosphorus concentration and speciation in urban wastewater for potential recovery. In *WASTES: Solutions, Treatments and Opportunities IV*; CRC Press: Boca Raton, FL, USA, 2023; ISBN 9781003345084.
22. Prot, T.; Korving, L.; Van Loosdrecht, M.C.M. Ionic strength of the liquid phase of different sludge streams in a wastewater treatment plant. *Water Sci. Technol.* **2022**, *85*, 1920–1935. [CrossRef] [PubMed]
23. Rodrigues, D.M.; do Amaral Fragoso, R.; Carvalho, A.P.; Hein, T.; de Brito, A.G. Are alternative magnesium sources the key for a viable downstream transfer of struvite precipitation? Assessment of process feasibility and precipitate characteristics. *J. Water Process Eng.* **2022**, *45*, 102508. [CrossRef]
24. Shaddel, S.; Grini, T.; Andreassen, J.-P.; Østerhus, S.W.; Ucar, S. Crystallization kinetics and growth of struvite crystals by seawater versus magnesium chloride as magnesium source: Towards enhancing sustainability and economics of struvite crystallization. *Chemosphere* **2020**, *256*, 126968. [CrossRef]
25. Ali, I.; Schneider, P.A. Crystallization of struvite from metastable region with different types of seed crystal. *J. Non-Equilib. Thermodyn.* **2005**, *30*, 95–111. [CrossRef]
26. Muhmood, A.; Lu, J.; Kadam, R.; Dong, R.; Guo, J.; Wu, S. Biochar seeding promotes struvite formation, but accelerates heavy metal accumulation. *Sci. Total Environ.* **2019**, *652*, 623–632. [CrossRef] [PubMed]
27. Rahaman, M.S.; Ellis, N.; Mavinic, D.S. Effects of various process parameters on struvite precipitation kinetics and subsequent determination of rate constants. *Water Sci. Technol.* **2008**, *57*, 647–654. [CrossRef] [PubMed]

28. Kim, D.; Ryu, H.-D.; Kim, M.-S.; Kim, J.; Lee, S.-I. Enhancing struvite precipitation potential for ammonia nitrogen removal in municipal landfill leachate. *J. Hazard. Mater.* **2007**, *146*, 81–85. [CrossRef] [PubMed]
29. Wang, J.; Burken, J.G.; Zhang, X. Effect of Seeding Materials and Mixing Strength on Struvite Precipitation. *Water Environ. Res.* **2006**, *78*, 125–132. [CrossRef] [PubMed]
30. Warmadewanthi; Liu, J.C. Recovery of phosphate and ammonium as struvite from semiconductor wastewater. *Sep. Purif. Technol.* **2009**, *64*, 368–373. [CrossRef]
31. Kim, D.; Min, K.J.; Lee, K.; Yu, M.S.; Park, K.Y. Effects of pH, molar ratios and pre-treatment on phosphorus recovery through struvite crystallization from effluent of anaerobically digested swine wastewater. *Environ. Eng. Res.* **2016**, *22*, 12–18. [CrossRef]
32. Lavanya, A.; Ramesh, S.T.; Nandhini, S. Phosphate recovery from swine wastewater by struvite precipitation and process optimization using response surface methodology. *Desalin. Water Treat.* **2019**, *164*, 134–143. [CrossRef]
33. Campos, P.V.; Angélica, R.S.; de Faria, L.J.G.; Paz, S.P.A. Da Phosphorus Recovery from Wastewater Aiming Fertilizer Production: Struvite Precipitation Optimization Using a Sequential Plackett–Burman and Doehlert Design. *Processes* **2023**, *11*, 2664. [CrossRef]
34. Yan, H.; Shih, K. Effects of calcium and ferric ions on struvite precipitation: A new assessment based on quantitative X-ray diffraction analysis. *Water Res.* **2016**, *95*, 310–318. [CrossRef]
35. Enyemadze, I.; Momade, F.W.Y.; Oduro-Kwarteng, S.; Essandoh, H. Phosphorus recovery by struvite precipitation: A review of the impact of calcium on struvite quality. *J. Water Sanit. Hyg. Dev.* **2021**, *11*, 706–718. [CrossRef]
36. Liu, X.; Wang, J. Impact of calcium on struvite crystallization in the wastewater and its competition with magnesium. *Chem. Eng. J.* **2019**, *378*, 122121. [CrossRef]
37. Battaz, S.; Djazi, F.; Allal, H.; Trabelsi, I.; Abdellah, Z.; Benrabaa, R.; Hamzaoui, A.H. Phosphorus recovery as struvite from wastewater by using seawater, brine and natural brine. *Desalin. Water Treat.* **2024**, *317*, 100082. [CrossRef]
38. Devatha, C.P.; Rashmi, H.R. Recovery of phosphorus as struvite from the dewatered liquor through crystallization using seawater as magnesium source. In *Resource Recovery in Municipal Waste Waters*; Elsevier: Amsterdam, The Netherlands, 2023; pp. 261–289.
39. Grini, T. Seawater as Magnesium Source for Struvite Crystallization in Wastewater—An Assessment of Seawater as an Alternative Magnesium Source of Struvite Production in Wastewater Treatment Plants. Master's Thesis, Norwegian University of Science and Technology, Trondheim, Norway, 2018.
40. Kabdasli, I.; Parsons, S.A.; Tunay, O. Effect of Major Ions on Induction Time of Struvite Precipitation. *Croat. Chem. Acta* **2006**, *79*, 243–251.
41. Kabdaşlı, I.; Tünay, O. Nutrient recovery by struvite precipitation, ion exchange and adsorption from source-separated human urine—A review. *Environ. Technol. Rev.* **2018**, *7*, 106–138. [CrossRef]
42. Wang, S.; Sun, K.; Xiang, H.; Zhao, Z.; Shi, Y.; Su, L.; Tan, C.; Zhang, L. Biochar-seeded struvite precipitation for simultaneous nutrient recovery and chemical oxygen demand removal in leachate: From laboratory to pilot scale. *Front. Chem.* **2022**, *10*, 990321. [CrossRef] [PubMed]
43. Chauhan, C.K.; Joshi, M.J. Growth and characterization of struvite-Na crystals. *J. Cryst. Growth* **2014**, *401*, 221–226. [CrossRef]
44. Gardner, L.J.; Walling, S.A.; Lawson, S.M.; Sun, S.; Bernal, S.A.; Corkhill, C.L.; Provis, J.L.; Apperley, D.C.; Iuga, D.; Hanna, J.V.; et al. Characterization of and Structural Insight into Struvite-K, $MgKPO_4{\cdot}6H_2O$, an Analogue of Struvite. *Inorg. Chem.* **2021**, *60*, 195–205. [CrossRef]
45. Huang, H.; Zhang, D.; Li, J.; Guo, G.; Tang, S. Phosphate recovery from swine wastewater using plant ash in chemical crystallization. *J. Clean. Prod.* **2017**, *168*, 338–345. [CrossRef]
46. Huang, H.; Zhang, D.; Wang, W.; Li, B.; Zhao, N.; Li, J.; Dai, J. Alleviating Na+ effect on phosphate and potassium recovery from synthetic urine by K-struvite crystallization using different magnesium sources. *Sci. Total Environ.* **2019**, *655*, 211–219. [CrossRef]
47. Watson, C.; Clemens, J.; Wichern, F. Hazenite: A new secondary phosphorus, potassium and magnesium fertiliser. *Plant Soil Environ.* **2020**, *66*, 1–6. [CrossRef]